ELSEVIER

Journal of Alloys and Compounds 434–435 (2007) 307–310

Journal of ALLOYS AND COMPOUNDS

www.elsevier.com/locate/jallcom

Deformation of nanocrystalline pure metals and alloys based on Fe and Al

N.I. Noskova

Institute of Metal Physics of UD Russian Academy of Science, Ekaterinburg, Russia

Abstract

Results of recent original studies of structure and properties of nanocrystalline metals and alloys produced by severe plastic deformation and by nanocrystallization of amorphous alloys are considered. High resolution transmission electron microscopy, scanning electron microscopy, and *in situ* deformation in the column of an electron microscope were used to analyze the structures and the mechanisms of plastic deformation of nanocrystalline materials.

Keywords: Nanostructured materials; Mechanical properties; Microstructure; Transmission electron microscopy

1. Introduction

Metals and alloys with structural parameters such as crystal grain, layer thickness of multilayers, diameter of a tube or a filament in multifilamentary composites, in the size range not exceeding 100 nm are considered as nanostructured materials. These materials can be produced by different processing methods, namely, evaporation–condensation of nanosized particles with further compaction, mechanical activation, super fast quenching from a melt with further crystallization, severe plastic deformation (SPD) [1–8]. The specific feature of the nanocrystalline materials is the fact that the volume fractions of atoms in grain boundary interlayers and grains bodies of the same order. Due to their unique strength and functional properties nanocrystalline materials arise much interest among material researchers. The present paper is aimed to analyze structural features, strength characteristics and plastic deformation mechanisms in a number of nanocrystalline materials.

2. Experimental

Nanocrystalline metals Ni, Cu, Fe, Ti and alloys Al + 0.1%Zr, Al + 1%Hf, Al + 0.5%Ce, Al + 0.2%Nb, Al + 1%Hf + 0.2%Nb + 0.2%Sn, Al + 0.5%Ce + 0.12%Zr + 0.5% were produced by severe plastic deformation (equal-channel angular pressing [1,3], and subsequent rolling in two directions [7], and rotation under pressure 5–8 GPa-deformation in Bridgman anvils [1]) and alloys ($Fe_{73.5}Cu_1Nb_3Si_{13.5}B_9$, $Fe_{60}Cr_{18}Ni_7Si_3B_{12}$ and $Fe_{60}Cr_{18}Ni_7Si_5B_{10}$) produced by nanocrystallization of amorphous alloys [1,8] were studied. The structure of nanocrystalline metals and alloys are analyzed by transmission electron microscopy JEM–200KX. Mechanical tests were performed on an Instron testing machine, the hardness of nanocrystalline materials were studied and *in situ* deformation in the column of an electron microscope was used to analyze the mechanisms of plastic deformation.

3. Results

3.1. Structural features of nanocrystalline metals and alloys

3.1.1. Pure metals

The investigation by transmission electron microscopy and by high resolution transmission electron microscopy have shown that nanocrystalline metals Ni, Cu produced by SPD, are characterized by a high level of internal distortions within a nanosized grain body which increase with near the grain boundary, and a non-equilibrium state of grain boundaries attributed to high dislocation density [1,9,10]. Nanocrystalline Mo and W by SPD possess “wider” grain boundary interlayers with high dislocation density than fcc-metals, which is most likely due to low dislocation mobility in bcc metals. Finally, nanocrystalline SPD processed Ti and Co have two types of boundaries in their structure, interphase and between similar grain that in turn result in different dislocation densities.

3.1.2. Alloys

The structure of nanosized grains and grain boundaries of nanocrystalline multiphase SPD processed alloys has been investigated in a number of publications [1,3,10–12]. Different processing schemes (modes) for formation of nanosized grains and phase generation in such alloys have were proposed

---

E-mail address: noskova@imp.uran.ru.

0925-8388/$ – see front matter © 2006 Elsevier B.V. All rights reserved.
doi:10.1016/j.jallcom.2006.08.185

Table 1
Microhardness (H), yield strength ($\sigma_{0.2}$) and ultimate tensile strength (σ_B) of SPD obtained poly- and nanocrystalline pure metals with different grain size (d) and relative elongation δ

Metal	d Change, nm (from–to)	H change, GPa (from–to)	$\sigma_{0.2}$ change, MPa (from–to)	σ_B change, MPa (from–to)	δ change, % (from – to)
Ti	50000–40	0.8–6.7	275–980	420–1310	29–5
Fe	10000–80	1.8–4.5	375–1010	480–1100	25–15
Cr	1500–70	–	313–780	485–960	–
Al	1500–200	0.3–1.2	13–26	42–176	20–2
Mo	500–50	1.0–6.0	–	–	–
W	200–40	3.0–6.2	–	–	–
Cu	200–70	0.9–1.4	60–365	120–650	60–30
Cu	70–20	1.4–1.8	–	–	–

in [12,13]. It is shown [10,14,15] that plastic deformation at high strains results in formation (transformation) of internal structure of different alloys by at least three ways (mechanisms), namely, continuous refining of structure, non-monotonous refining with a “threshold” of internal elastic distortions overcoming of which results in structure refining and combination of phase formation and structure refining.

3.2. Mechanical properties of nanocrystalline materials

Mechanical properties of nanocrystalline materials are determined mainly by the nanograin size d and the state of nanograin boundaries. Thus, with decreasing d from 1500 to 5 nm the microhardness H of pure metals may increase by a factor of 2–6 [1,13] (Table 1). The yield strength $\sigma_{0.2}$ and ultimate tensile strength σ_B of nanocrystalline metals also grow compared to those of the coarse grain state, while the low temperature plasticity δ decreases.

For nanocrystalline metals copper, armco-iron and titanium with fcc, bcc and hcp crystal structure, extension and slope of the linear elastic portion of the diagram increase drastically. For nanocrystalline Fe with a grain size of 40 nm the “yield tooth” and the “yield flat” disappear and the extension of the linear elastic portion of the tensile diagram increases. In the majority of cases the plasticity of pure nanocrystalline metals at low testing temperatures is lower than that of conventional polycrystals (Table 1).

The Hall–Petch relation $\sigma_{0.2} = \sigma_o + kd^{-0.5}$, where σ_0 is the lattice friction, $k = f(G,b)$, G the shear modulus and b is Burger’s vector modulus, for nanocrystalline materials may be extended to microhardness, namely, $H = f(kd^{-0.5})$. Numerous experiments to check this dependence in nanocrystalline pure metals [1,6] have shown that it is not valid within the whole range of $d = (2–100\text{ nm})$ and strongly depends on the method for processing nanocrystals (Table 1). Researchers assume that the deviation from the Hall–Petch law at small grain sizes is connected with modification of deformation mechanism. This assumption is possible, since it is known that the stress needed to activate a dislocation source is rather high in a nanosized grain, e.g. for Ni with a grain size (dislocation source size) of 140 nm it is 870 MPa, the shear modulus of nickel being 95 MPa.

Mechanical properties of some nanocrystalline multiphase alloys are presented in Table 2. It is seen that in alloys, as in pure metals, the transition to a structure with sub-micron or nanosized grains is accompanied by increase of microhardness and strength. Besides, superplasticity appears at high temperatures [1]. Similar to pure nanocrystalline metals, the Hall–Petch dependence for nanophase alloys is not valid within the whole nanophase size range [1]. In most cases the Hall–Petch law is not valid for alloys with a grain size of 30 nm and less, the coeffi-

Table 2
Nanograin size (d), microhardness (H), yield strength ($\sigma_{0.2}$), ultimate tensile strength (σ_B) and relative elongation (δ) of coarse-crystalline and nanocrystalline SPD obtained alloys

Alloy	d Change, nm (from–to)	H change, GPa (from–to)	$\sigma_{0.2}$ change, MPa (from–to)	σ_B change, MPa (from–to)	δ change,% (from–to)
FeCuNbSiB	200–6	6.0–15.0	140–2180	140–2280	0–0.8
CoFeSiB	100–25	10.5–13.0	945–1880	950–2100	0–2.6
	25–8	13.0–9.0	–	–	–
Fe–12%Cr–18%Ni–10%Ti	3000–150	–	500–1600	–	–
Fe–12%Cr–25%Ti	2000–50	1.8–6.5	–	1500–2500	–
AlNiCeFe	2000–80	–	–	120–1560	–
Al–1%Hf	2500–760	0.3–0.4	30–160	40–180	
Al–1%Hf–0.2%Nb–0.2%Sn	2000–110	0.4–0.8	40–140	60–200	0.3–4.8
	110–60	0.8–1.8	–	–	–
Al–0.5%Ce–0.5%Re–0.1%Zr	2000–150	0.4–0.65	40–180	80–220	0.1–5.2
	120–40	1.0–1.9	–	–	–
Ni_3Al	1000–60	–	–	780–3000	–

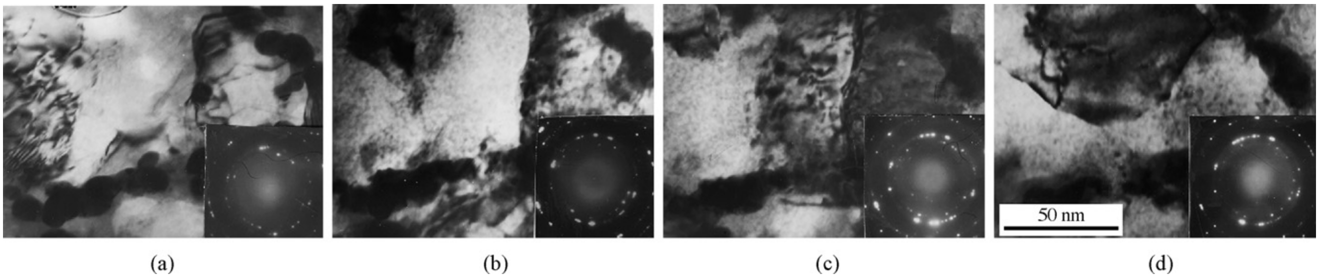

Fig. 1. Successive TEM images of one and the same area of nanocrystalline Al + 1%Hf alloy ($d = 60$ nm) deformed in the electron-microscope column with relative elongation δ: (a) strain $\delta = 9.0\%$; (b) $\delta = 14.5\%$; (c) $\delta = 24.5$; (d) $\delta = 36.8\%$.

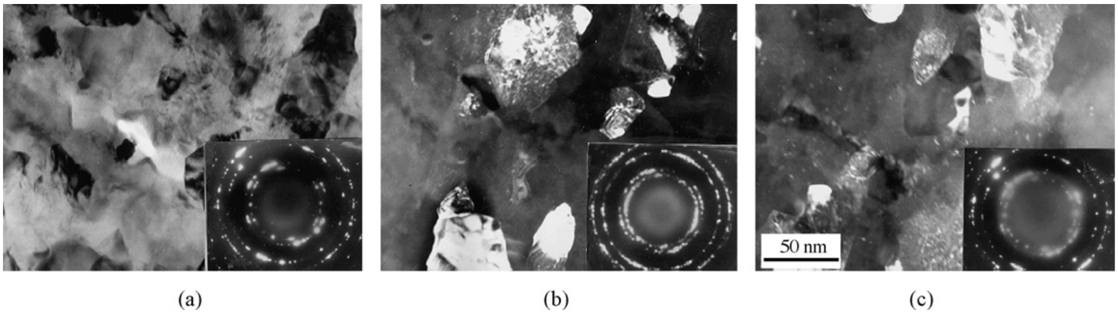

Fig. 2. TEM successive images of one and the same area of nanocrystalline alloy Al–0.5%Ce–0.5%Re–0.1%Zr ($d = 40$ nm) deformed in the electron-microscope column with relative elongation δ: (a) strain $\delta = 9.0\%$; (b) $\delta = 24.5\%$; (c) $\delta = 67.5\%$.

cient k having a negative value. The possible causes for violation of the Hall–Petch law for nanocrystalline alloys are the same as for pure metals, namely, modification of the plastic deformation mechanism and the weakening of nanograin boundaries.

3.3. Plastic deformation mechanism of nanocrystalline materials

The results of "*in situ*" deformation investigations [1,13–15] show that tensile deformation of nanocrystalline nickel with the grain size of 40–70 nm is realized both through dislocation creep (slip, sliding) and nanograin rotation. There arise dislocation pile-ups near grain boundaries in coarser grains. In fine nanograins, dislocations are immobile and nanograins undergo rotation which, as a rule, is accompanied by the growth of density of grain boundary dislocations and formation of a deformation band along grain boundaries of a number of nanograins.

Deformation of nanocrystalline copper with a grain size of 30 nm is realized mainly through rotation of grains relative to each other. It was determined that grains rotation relative to each other occurs through angles from 0.5° to 30° with increasing strain from zero up to failure. The rotation of nanograins is caused by internal stresses which are accumulated and concentrated in triple junctions of nanograins and are rearranged and partially decreased by rotation.

During deformation of nanocrystalline copper the dislocations observed within the grain interior remain immobile. At the same time the amount of defects at nanograin boundaries appreciably increases and nanograin boundaries become "broader" that indicating the active character of deformation processes occurring along nanograin boundaries. The rotation of nanograins is most likely accompanied by the occurrence of discontinuities along grain boundaries.

Figs. 1a–d and 2a–c demonstrate transmission electron microscope images of one and the same site of microstructure of Al + 1%Hf (Fig. 1), and Al–0.5%Ce–0.5%Re–0.1%Zr (Fig. 2) nanocrystalline alloys subjected to tensile deformation at different strain values δ increased successively ("*in situ*" method). As seen from Figs. 1 and 2, deformation occurs by the dislocation-rotation mechanism (with increasing strain value there occurs a rotation of nanograins and the density of grain boundary dislocations increases). Particles of a phase, not more than 10 nm in size, are observed at nanograins boundaries. With strain, particles both retard the movement of dislocations, and interacting with grain boundary dislocations, undergo "dissolution". Concurrently there occurs formation of finely dispersed phases within the nanograin interior that results in strengthening of nanograins.

The view of deformation process in a nanocrystalline material through nanograins rotation and nanograins displacement along boundaries is apparently close to the real mechanism of deformation. One should take into account dependence of strength and plasticity on concentration of the second nanophase in a nanocrystalline alloy forming in the process of its deformation, because elastic modulus changes appreciably with change in the quantitative ratio of matrix to second phase volume fractions.

4. Conclusion

The grain size refinement to several tens of nanometers in nanocrystalline metals and alloys is accompanied by considerable growth of their strength and hardness.

The"*in situ*" study of deformation of fcc, bcc and hcp nanocrystalline materials made it possible to conclude that during tensile deformation resulting in a decrease of a nanograin size, there occur rotation modes which due to their cooperative character cause the development of mesoscopic deformation shifts at grain boundaries. Development of the rotation deformation modes in nanocrystalline materials leads to initiation of rotation plasticity in the form of grain boundary mesoscopic shifts.

Acknowledgment

This work was supported by the Russian Foundation for Basic Research, grant no. 04-02-17874.

References

[1] N.I. Noskova, R.R. Mulyukov, Submicrocrystallin and Nanocrystallin Metals and Alloys, UrD RAS, Ekaterinburg, 2003 (in Russian).

[2] I.D. Morokhov, L.I. Trusov, V.I. Lapovok, Physical Phenomena in Ultra-Fine Environments., Nauka, Moscow, 1984 (in Russian).

[3] N.A. Akhmadeev, N.P. Kobelev, R.R. Mulyukov, Ya.M. Soifer, R.Z. Valiev, Acta Metall. Mater. 41 (1993) 1041–1046.

[4] R. Birringer, H. Gleiter, in: R.W. Cahn (Ed.), Encyclopedia of Materials Science and Engineering, Suppl.1, Pergamon Press, 1988, pp. 339–348.

[5] H. Fecht, J. Nanostruct. Mater. 1 (1995) 33–42.

[6] V.G. Gryaznov, L.I. Trusov, Prog. Mater. Sci. 37 (1993) 290–400.

[7] N.I. Noskova, I.A. Pereturina, V.V. Stolyarov, O.A. Elkina, J. Phys. Met. Metallogr. 97 (2004) 531.

[8] U. Koster, U. Schunemann, M. Blank-Bewersdorff, S. Braner, M. Sutton, G.B. Stephenson, J. Mater. Sci. Eng. A133 (1991) 611–615.

[9] D. Wolf, M.D. Klude, Scr. Met. At. Mater. 24 (1990) 907–912.

[10] N.I. Noskova, E.G. Ponomareva, M.M. Myshlyaev, J. Phys. Met. Metallogr. 83 (1997) 511–513.

[11] N. Noskova, R. Andrievski, V. Ivanov, J. Metastable Nanocryst. Mater. 307 (1999) 211–216.

[12] N.I. Noskova, A.V. Korznikov, S.R. Idrisova, J. Phys. Met. Metallogr. 89 (2000) 103–110.

[13] N.I. Noskova, J. Phys. Met. Metallogr. 94 (Suppl. 1) (2002) S119–S130.

[14] N.I. Noskova, E.I. Volkova, J. Phys. Met. Metallogr. 91 (2001) 629–635.

[15] N.I. Noskova, E.G. Volkova, J. Phys. Met. Metallogr. 92 (2001) 421–425.